FEBS Letters

FEBS PRESS science publishing by scientists

Receptor-Interacting Protein Kinase 3 (RIPK3) inhibits autophagic flux during necroptosis in intestinal epithelial cells

Kana Otsubo[1], Chiaki Maeyashiki[1], Yoichi Nibe[1], Akiko Tamura[1], Emi Aonuma[1], Hiroki Matsuda[1], Masanori Kobayashi[1], Michio Onizawa[1], Yasuhiro Nemoto[1], Takashi Nagaishi[2], Ryuichi Okamoto[3], Kiichiro Tsuchiya[1], Tetsuya Nakamura[4], Satoru Torii[5], Eisuke Itakura[6], Mamoru Watanabe[1,7] and Shigeru Oshima[1]

1 Department of Gastroenterology and Hepatology, Graduate School, Tokyo Medical and Dental University, Japan
2 Department of Advanced Therapeutics for GI Diseases, Tokyo Medical and Dental University, Japan
3 Center for Stem Cell and Regenerative Medicine, Tokyo Medical and Dental University, Japan
4 Department of Research and Development for Organoids, Juntendo University School of Medicine, Tokyo, Japan
5 Department of Pathological Cell Biology, Medical Research Institute, Tokyo Medical and Dental University, Japan
6 Department of Biology, Graduate school of Science, Chiba University, Japan
7 Advanced Research Institute, Tokyo Medical and Dental University, Japan

Correspondence
S. Oshima, Department of Gastroenterology and Hepatology, Graduate School, Tokyo Medical and Dental University, 1-5-45, Yushima, Bunkyo-Ku, Tokyo 113-8519, Japan
Tel: +81 3 5803 5877
E-mail: soshima.gast@tmd.ac.jp

Kana Otsubo and Chiaki Maeyashiki contributed equally to this article.

(Received 19 December 2019, revised 17 January 2020, accepted 20 January 2020, available online 16 February 2020)

doi:10.1002/1873-3468.13748

Edited by Barry Halliwell

Autophagy is an intracellular process that regulates the degradation of cytosolic proteins and organelles. Dying cells often accumulate autophagosomes. However, the mechanisms by which necroptotic stimulation induces autophagosomes are not defined. Here, we demonstrate that the activation of necroptosis with TNF-α plus the cell-permeable pan-caspase inhibitor Z-VAD induces LC3-II and LC3 puncta, markers of autophagosomes, via the receptor-interacting protein kinase 3 (RIPK3) in intestinal epithelial cells. Surprisingly, necroptotic stimulation reduces autophagic activity, as evidenced by enlarged puncta of the autophagic substrate SQSTM1/p62 and its increased colocalization with LC3. However, necroptotic stimulation does not induce the lysosomal-associated membrane protein 1 (LAMP1) nor syntaxin 17, which mediates autophagosome–lysosome fusion, to colocalize with LC3. These data indicate that necroptosis attenuates autophagic flux before the lysosome fusion step. Our findings may provide insights into human diseases involving necroptosis.

Keywords: autophagy; necroptotic stimulation; necrostatin-1; RIPK3; SQSTM1/p62; STX17

Autophagy is an intracellular degradation process that delivers cytoplasmic materials to lysosomes [1]. It is an essential process that maintains cellular and tissue homeostasis. Following autophagy induction, the isolation membrane encloses a small portion of the cytoplasm and then closes. This forms a double-membrane structure termed the autophagosome. LC3 is conjugated to phosphatidylethanolamine to form LC3-II, which is localized to isolation membranes and autophagosomes. ATG16L1 plays a pivotal role in canonical autophagy processes and is recruited to the isolation membrane. When an endosome fuses with an

Abbreviations
LAMP1, lysosomal-associated membrane protein 1; LC3/MAP1LC3, microtubule-associated protein 1 light chain 3; PBS, phosphate-buffered saline; SQSTM1/p62, sequestosome 1; STX17, syntaxin 17; TNF-α, tumor necrosis factor-α; Z-VAD, Z-Val-Ala-DL-Asp(OMe)-FMK.

autophagosome, it results in the formation of an amphisome. The autophagosome or the amphisome fuses with the lysosome to form the autolysosome and degrade internal contents [2]. At the time of starvation in mammals, syntaxin 17 (STX17) is recruited to the autophagosome and mediates autophagosome–lysosome fusion. Therefore, depleting STX17 causes the accumulation of autophagosomes. Lysosomal-associated membrane protein 1 (LAMP1) is distributed among autophagic and endolysosomal organelles. LAMP1-positive organelles are often referred to as lysosomal compartments. Sequestosome 1 (SQSTM1/p62) is a ubiquitous protein that is regulated through stress-responsible transcription factors [3]. It targets ubiquitinated cargo, including aggregates, damaged mitochondria, and microbes, for selective autophagy [4]. SQSTM1/p62 binds to polyubiquitin via its C-terminal ubiquitin-associated domain [5] and LC3, where it is degraded by autophagy. It has been observed that SQSTM1/p62 accumulates when autophagy is inhibited, but decreases when autophagy is induced. Autophagic flux is often defined as a measure of autophagic degradation activity. Hence, the degradation of SQSTM1/p62 is widely used as a marker to monitor autophagic flux.

Necroptosis is a genetically regulated form of necrotic cell death [6–8] that can be induced by the addition of TNF-α to caspase-8 inhibited cells. Inactivation of caspase-8 by chemical inhibitors, such as the cell-permeable pan-caspase inhibitor Z-VAD, as well as FADD or caspase-8 deficiency, prevents the cleavage of receptor-interacting protein kinase 1 (RIPK1) to permit the activation of necroptosis in cells stimulated by TNF-α. RIPK1/RIPK3, critical mediators of necroptosis, has been implicated in various human diseases [9–12]. Several studies have indicated that human RIPK1 deficiency can result in intestinal inflammation [13,14]. RIPK1, RIPK2, and RIPK3 function is essential for cell death and inflammation, which is regulated by TNFAIP3/A20 [15–17]. Dying cells often accumulate autophagosomes [18], which may be termed 'cell death with autophagy' rather than 'cell death by autophagy'. [19]. Previous studies have shown that necroptosis signals induce autophagy [20–24]. Specifically, it has been demonstrated that RIPK3 regulates the formation of the SQSTM1/p62-LC3 complex, which is regulated by caspase 8 and TNFAIP3/A20 [25]. However, the TNF-α stimulation-dependent LC3-II accumulation mechanism is poorly understood. A recent paper demonstrated that LC3-II accumulation during necroptosis occurs independently of autophagy activation in mouse dermal fibroblasts [23]. Here, we demonstrate that necroptotic stimulation with TNF-α plus Z-VAD increases LC3-II and LC3 puncta but does not induce autophagic flux in intestinal epithelial cells.

Materials and methods

Cell culture and reagents

Cells from the human colorectal cancer cell lines HT29 and HCT116 were cultured in Dulbecco's modified Eagle medium (D5796; Sigma-Aldrich, St. Louis, MO, USA) with 10% fetal bovine serum (S1820; Biowest SAS, Nuaillé, France) and 1% penicillin/streptomycin (26253-84; Nacalai Tesque, Inc., Kyoto, Japan) at 37°C. Cells were transiently transfected with plasmids using Lipofectamine 2000 (11668019; Invitrogen, Carlsbad, CA, USA) following the manufacturer's instructions. Recombinant human TNF-α (300-01A; PeproTech Corp., Rocky Hill, NJ, USA) was dissolved in RNase-free water at a concentration of 100 $\mu g \cdot mL^{-1}$ for a final concentration of 50 $ng \cdot mL^{-1}$. Z-VAD (3188-V; Peptide Institute, Inc., Osaka, Japan) and necrostatin-1 (Nec-1; RIPK1-specific inhibitor; 480065; Sigma-Aldrich) were dissolved in dimethyl sulfoxide at a concentration of 50 mM for a final concentration of 50 μM. Torin-1 (42427; Tocris Bioscience, Bristol, UK) was dissolved in dimethyl sulfoxide to a final concentration of 50 nM. MG-132 (tlrl-mh132; InvivoGen, San Diego, CA, USA) was dissolved in dimethyl sulfoxide to a final concentration of 5 μM. Mouse Ripk3 cDNA was cloned into pCR3.1 2XFLAG. Myc-human RIPK3 and MRX-IP GFP-STX17 plasmids have been described previously [2,25].

Microscopy analysis

Cells were washed with phosphate-buffered saline (PBS; 14249–24; Nacalai Tesque, Inc.) and fixed in 4% paraformaldehyde (09154–85; Nacalai Tesque, Inc.) for 10 min at 4 °C. Fixed cells were then washed with PBS, permeabilized with 50 $\mu g \cdot mL^{-1}$ digitonin (BN2006; Invitrogen) in PBS for 5 min, and then blocked with 3% bovine serum albumin (01863–48; Nacalai Tesque, Inc.) in PBS for 30 min. Cells were then incubated for 1 h with anti-LC3 (M152-3; MBL International Corporation, Nagoya, Japan), anti-c-Myc (A-14; sc-789; Santa Cruz Biotechnology, Inc., Dallas, TX, USA), anti-Myc-Tag (71D10; 2278; Cell Signaling Technology, Inc., Danvers, MA, USA), anti-FLAG (F7425; Sigma-Aldrich), anti-SQSTM1/p62 (PM045; MBL International Corporation), anti-LAMP1 (ab24170; Abcam, Cambridge, UK), or anti-ATG16L1 (D6D5; 8089; Cell Signaling Technology). After washing, cells were incubated with Alexa Fluor 488-conjugated anti-mouse secondary antibody (A11001; Invitrogen), 488-conjugated anti-rabbit antibody (A21206; Invitrogen), 594-conjugated anti-mouse secondary antibody (A21203; Invitrogen), or 594-

conjugated anti-rabbit antibody (A21207; Invitrogen) for 1 h. The nucleolus was stained using VECTASHIELD® Mounting Medium with DAPI (H-1200; Vector Laboratories, Inc., Burlingame, CA, USA). For aggresome detection, ProteoStat® aggresome detection dye (ENZ-51035-0025; Enzo Life Sciences, Inc., Farmingdale, NY, USA) was used according to the manufacturer's protocol with minor modifications (permeabilizing solution, 5% Digitonin). Cells were incubated with anti-SQSTM1/p62 (PM045; MBL International Corporation) for 1 h. After washing in PBS, cells were incubated with Alexa Fluor 647-conjugated anti-rabbit secondary antibody (A32733; Invitrogen), washed again with PBS, and stained with ProteoStat® aggresome detection dye for 30 min at room temperature. A Texas Red filter set was used to view the ProteoStat® dye. Images were acquired using a confocal laser microscope (FV10i; Olympus Corp., Tokyo, Japan) with a 60× oil-immersion objective lens. The numbers of puncta per cell were counted manually or processed using IMAGEJ software (National Institutes of Health, Bethesda, MD, USA) for quantitative analysis.

Immunoblotting

HT29 cells were incubated in lysis buffer [20 mM Tris/HCl, pH 7.5; 150 mM NaCl; 0.2% NP-40 (23640–65; Nacalai Tesque, Inc.); 10% glycerol; and protease and phosphatase inhibitor cocktail] on ice for 20 min and then centrifuged at 14 000 ***g*** for 20 min. Samples were resolved on NuPAGE precast 4–12% Bis/Tris gels (NP0323; Invitrogen) and transferred to polyvinylidene difluoride membranes. The following antibodies and reagents were used for immunoblotting studies: anti-β-actin (A5441; Sigma-Aldrich), anti-LC3 (M152-3; MBL International Corporation), and anti-SQSTM1/p62 (PM045; MBL International Corporation). Secondary antibodies [mouse anti-rabbit (211-032-171) and goat anti-mouse (115-035-174)] were purchased from Jackson ImmunoResearch Inc. (West Grove, PA, USA).

Statistical analysis

Data are expressed as the mean ± standard deviation. Statistical significance was calculated using an unpaired Student's *t* test or one-way ANOVA followed by Tukey's test. Statistical analysis was performed using PRISM 5.0 (GraphPad, San Diego, CA, USA).

Results

TNF-α plus Z-VAD stimulation induced LC3 puncta in intestinal epithelial cells

To investigate whether necroptosis stimulation mediated autophagy in intestinal epithelial cells, we used TNF-α plus Z-VAD as a necroptotic stimulation [7,8,10,12]. HT29 cells, expressing endogenous RIPK3, were stimulated with TNF-α plus Z-VAD, and LC3 conversion was analyzed. The LC3-II form was increased in a time-dependent manner in HT29 cells (Fig. 1A). The LC3 puncta formation assay was performed to confirm whether increases in the LC3-II form were due to an increase in autophagosomes. Microscopic analysis reveals that TNF-α plus Z-VAD stimulation increased LC3 puncta (Fig. 1B,C). To understand the role of RIPK1/RIPK3 in LC3 puncta formation, cells were treated with the RIPK1 inhibitor Nec-1 [20]. Without necroptosis stimulation, Nec-1 treatment reduced LC3 puncta compared with no treatment. Therefore, baseline LC3 puncta may be influenced by endogenous RIPK1/RIPK3 expression. Further, LC3 puncta induced by TNF-α plus Z-VAD were suppressed by Nec-l treatment. These data indicate that TNF-α plus Z-VAD induced LC3 puncta through RIPK1/RIPK3 in HT29 cells.

Next, the intestinal epithelial cell line HCT116, which lacks RIPK3 expression [26], was used to clarify the role of RIPK3 in the increased LC3 puncta observed following TNF-α plus Z-VAD treatment. To confirm RIPK3 dependency of this phenomenon, Myc-RIPK3 was introduced into HCT116 cells and the LC3 puncta in Myc-expressing cells were analyzed (Fig. 1D). Although LC3 puncta were not increased when cells stimulated by TNF-α plus Z-VAD were treated with a control vector, the introduction of Myc-RIPK3 enhanced LC3 puncta stimulated by TNF-α plus Z-VAD. Furthermore, RIPK3 kinase-dead mutant (K51A) did not induce LC3 puncta (Fig. 1E). Taken together, these data indicate that TNF-α plus Z-VAD stimulation induces LC3 puncta via RIPK3 in intestinal epithelial cells.

TNF-α plus Z-VAD stimulation enlarged the puncta size of SQSTM1/p62 via RIPK3

SQSTM1/p62 protein is primarily known as a mediator of selective autophagy. SQSTM1/p62 localizes to cargo and degrades when autophagy flux is increased [3,4]. Therefore, SQSTM1/p62 protein expression was examined in HT29 cells using immunoblotting (Fig. 2A). Surprisingly, increased SQSTM1/p62 expression was observed after TNF-α plus Z-VAD stimulation. Confocal microscopy revealed that SQSTM1/p62 puncta size increased in a stimulus-dependent manner (Fig. 2B). These data indicate that TNF-α plus Z-VAD-induced LC3 puncta are not simply a result of autophagy flux. The RIPK3-deficient HCT116 cells were used to further examine the role of RIPK3 in

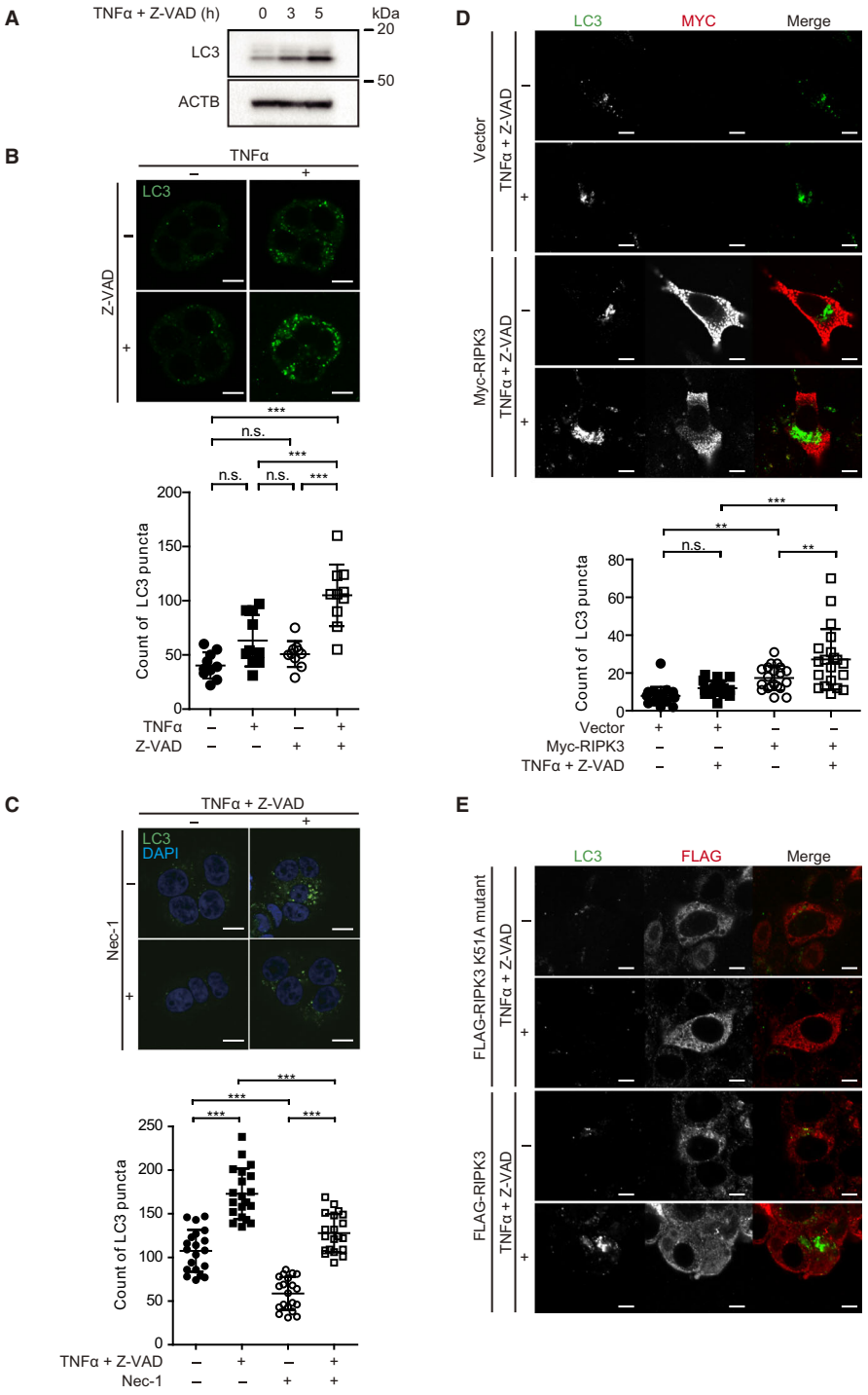

Fig. 1. TNF-α plus Z-VAD stimulation induced LC3 puncta in intestinal epithelial cells. (A) LC3 conversion assay. HT29 cells were treated with TNF-α (50 ng·mL^{-1}) plus Z-VAD (50 μM), cells were lysed, and protein extracts were immunoblotted for the indicated proteins. (B) HT29 cells were stimulated with TNF-α, Z-VAD, or TNF-α plus Z-VAD for 12 h and were stained with anti-LC3 antibody. n = 10 per group. (C) LC3 puncta formation assay. HT29 cells were stimulated with TNF-α plus Z-VAD alone, Nec-1 alone, or TNF-α plus Z-VAD and Nec-1 (50 μM) for 3 h. HT29 cells were stained with anti-LC3 antibody. (D) HCT116 cells were transfected with Myc-tagged human RIPK3 plasmids or empty vector for 48 h and stimulated with TNF-α plus Z-VAD for the last 3 h. HCT116 cells were stained with anti-c-Myc and anti-LC3 antibodies. Data are shown as mean ± SD, n = 20 per group. ** indicates $P < 0.01$, and *** indicates $P < 0.001$. Scale bars indicate 10 μm. Data are representative of three independent experiments. (E) HCT116 cells were transfected with FLAG-tagged mouse RIPK3 plasmids or RIPK3 K51A mutant (kinase-dead mutant) for 48 h and stimulated with TNF-α plus Z-VAD for the last 3 h. HCT116 cells were stained with anti-FLAG and anti-LC3 antibodies.

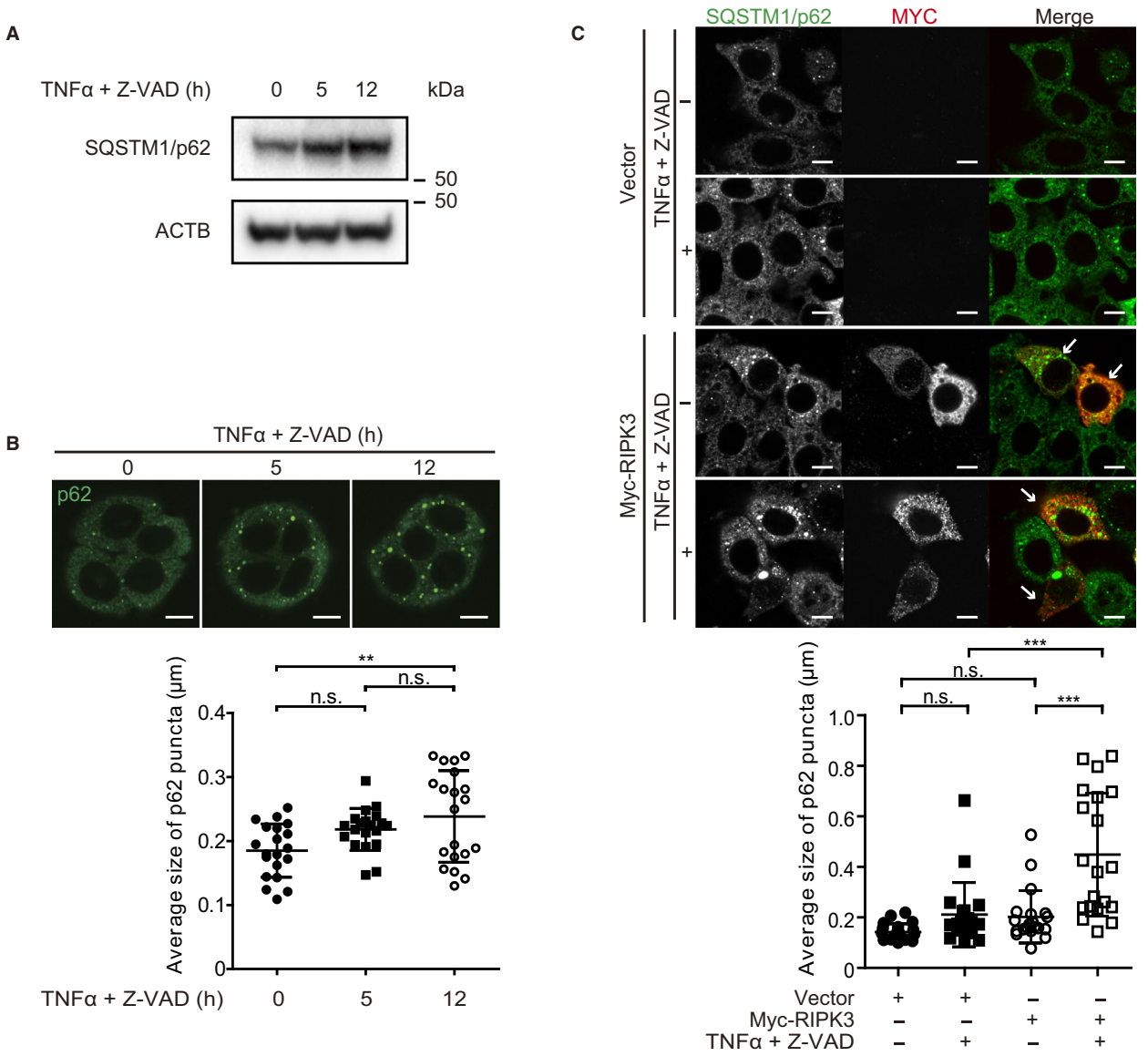

Fig. 2. TNF-α plus Z-VAD stimulation enlarges SQSTM1/p62 puncta size via RIPK3. (A) Immunoblot analysis in HT29 cells. HT29 cells were stimulated with TNF-α plus Z-VAD, cells were lysed, and protein extracts were immunoblotted for the indicated proteins. (B) HT29 cells were stimulated with TNF-α plus Z-VAD and stained with anti-SQSTM1/p62 antibody. (C) HCT116 cells were transfected with Myc-tagged human RIPK3 plasmids or empty vector for 48 h, then stimulated with TNF-α plus Z-VAD for the last 12 h, and stained with anti-c-Myc antibody and anti-SQSTM1/p62 antibody. Data are shown as mean ± SD, $n = 20$ per group. ** indicates $P < 0.01$, and *** indicates $P < 0.001$. Scale bars indicate 10 μm. Data are representative of independent experiments.

SQSTM1/p62 puncta (Fig. 2C). SQSTM1/p62 puncta size was measured in HCT116 cells transfected with Myc-RIPK3. SQSTM1/p62 puncta sizes were not increased when cells stimulated by TNF-α plus Z-VAD were treated with a control vector. Surprisingly, SQSTM1/p62 puncta size was increased in a stimulus-dependent manner in RIPK3-transfected cells. These results indicate that TNF-α plus Z-VAD stimulation simultaneously enhanced LC3 puncta expression and SQSTM1/p62 puncta size in a RIPK3-dependent manner. These data also indicate that necroptotic stimulation might block autophagy flux.

TNF-α plus Z-VAD stimulation enhanced SQSTM1/p62-LC3, but not aberrant aggresome

Upon the induction of autophagy, a small portion of the cytoplasm is enclosed by the isolation membrane.

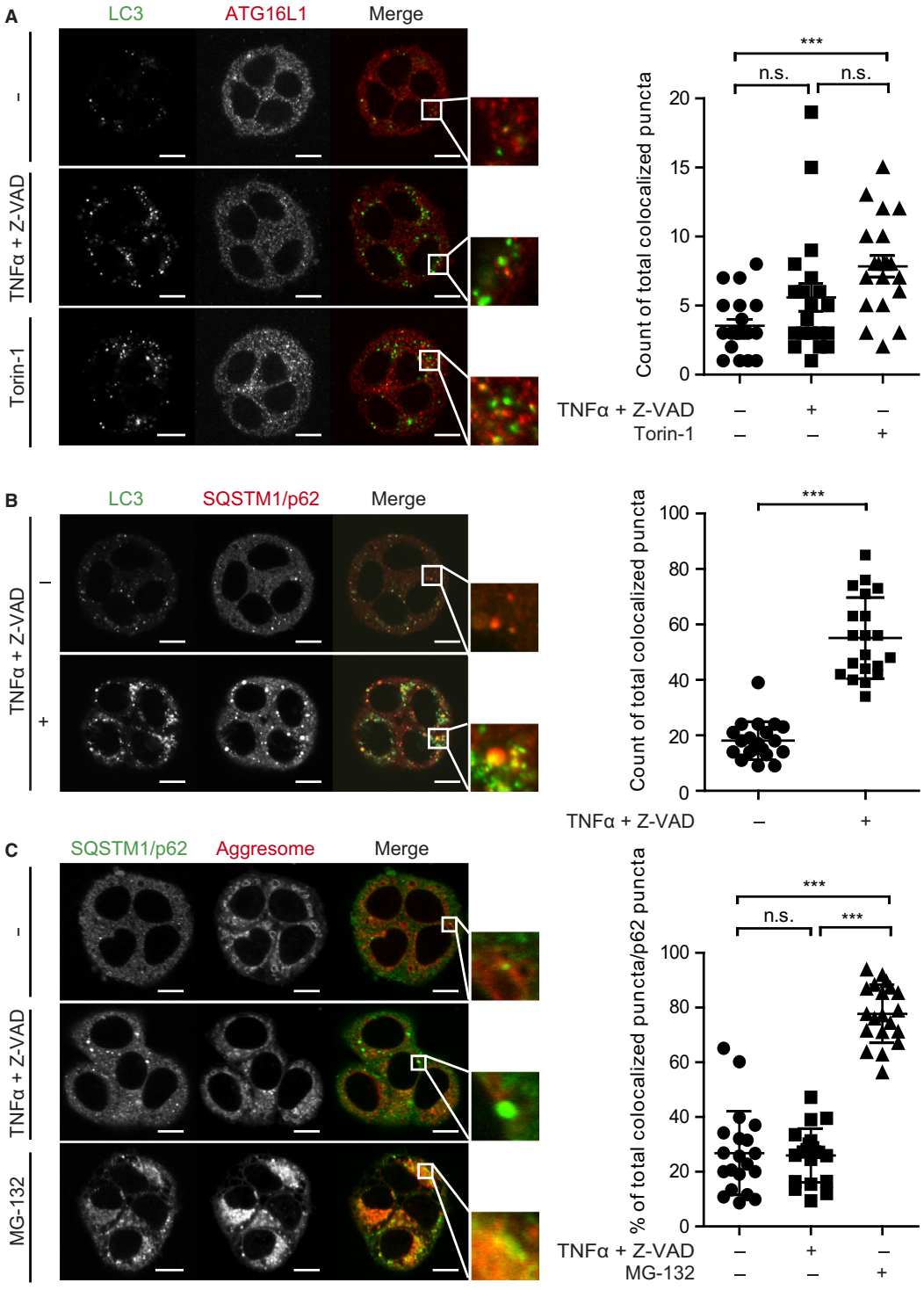

Fig. 3. TNF-α plus Z-VAD stimulation enhanced SQSTM1/p62-LC3 but not aberrant aggresome. (A) HT29 cells were stimulated with TNF-α plus Z-VAD or Torin-1 (50 nM) for 1 h and stained with anti-LC3 and anti-ATG16L1 antibodies. (B) HT29 cells were stimulated with TNF-α plus Z-VAD for 12 h and stained with anti-LC3 and anti-SQSTM1/p62 antibodies. (C) HT29 cells were stimulated with TNF-α plus Z-VAD or MG-132 (5 μM) for 12 h and stained with anti-SQSTM1/p62 antibody and ProteoStat aggresome detection dye. Data are shown as mean ± SD, $n = 20$ per group. *** indicates $P < 0.001$. Scale bars indicate 10 μm. Data are representative of independent experiments.

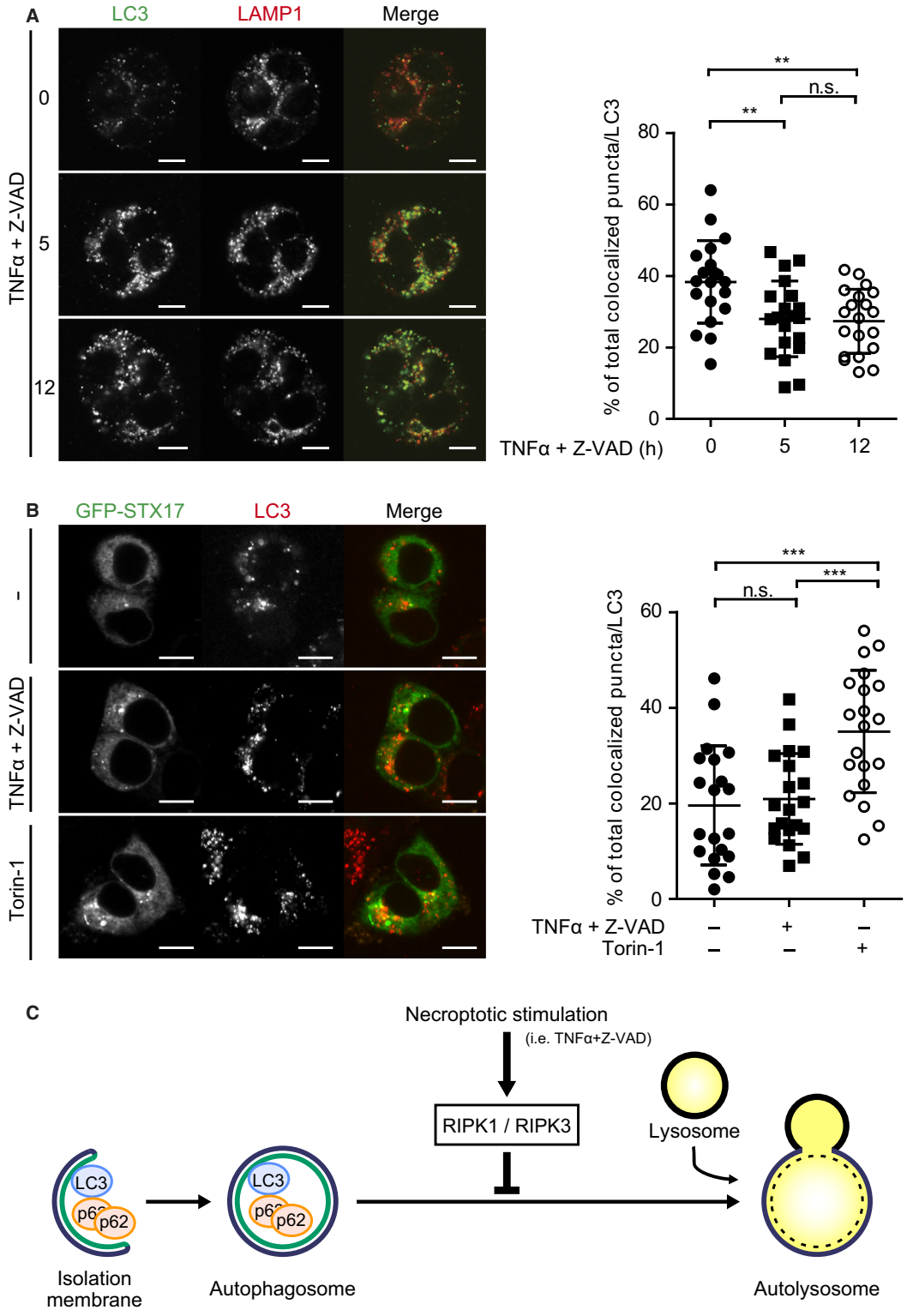

Fig. 4. Autophagy flux is attenuated before the lysosome fusion step in necroptosis-induced cells. (A) HT29 cells were stimulated with TNF-α plus Z-VAD for 12 h and stained with anti-LC3 and anti-LAMP1 antibodies. (B) Immunocytochemical assay in HT29 cells. Cells were transfected with pMRX-IP GFP-STX17 plasmid for 42 h and stimulated with TNF-α plus Z-VAD or Torin-1 for the last 12 h. Cells were stained with anti-LC3 antibody. (C) A model of RIPK3 inhibition of autophagic flux during necroptosis. Data are shown as mean ± SD, $n = 20$ per group. ** indicates $P < 0.01$, *** indicates $P < 0.001$. Scale bars indicate 10 μm. Data are representative of independent experiments.

To detect the isolation membrane, we analyzed ATG16L1-LC3 colocalization (Fig. 3A). As a positive control of autophagy activation, cells were stimulated with Torin-1, which is a potent and selective mTOR inhibitor [27]. We found increased ATG16L1-LC3 colocalization after 1-h treatment with Torin-1 but not with TNF-α and Z-VAD. Although the possibility remains that TNF-α and Z-VAD may induce ATG16L1-LC3 colocalization at a different time point, no colocalization occurred at this time point. To investigate autophagy flux, colocalization of SQSTM1/p62 and LC3 puncta was observed (Fig. 3B). Microscopic analysis revealed increased SQSTM1/p62-LC3 puncta colocalization in HT29 cells following TNF-α plus Z-VAD treatment, indicating that necroptotic stimulation may block degradation of SQSTM1/p62 and LC3. SQSTM1/p62 localizes to cargo fated for degradation during autophagy. Therefore, to address the possibility that SQSTM1/p62-LC3 puncta might be aberrant aggregates (not necessarily autophagosomes) formed in dying cells, we stained SQSTM1/p62 with aggresome detection dye (Fig. 3C). As a positive control, aggresomes were induced in HT29 cells by stimulation with the proteasome inhibitor MG-132. After MG-132 stimulation, SQSTM1/p62 proteins strongly accumulated, and SQSTM1/p62 and aggresome detection dye strongly colocalized. However, we did not observe the induction of SQSTM1/p62 aggresome colocalization following TNF-α and Z-VAD treatment. These data suggest that SQSTM1/p62-LC3 double-positive areas are not aberrant aggregates at this time point. Taken together, these data indicate that necroptotic stimulation may decrease the degradation of SQSTM1/p62 and LC3.

Autophagy flux is attenuated before the lysosome fusion step in necroptosis-induced cells

A previous study showed that necroptosis pathway may reduce autolysosomal function [23]. Therefore, necroptotic stimulation may control fusion of the autophagosome or amphisome and lysosome. To investigate this process, colocalization of the lysosome marker LAMP1 with LC3 was quantified in HT29 cells (Fig. 4A). Although the total number of LC3 puncta was increased (Fig. 1B), the percent of LAMP1-LC3 colocalization was not altered following TNF-α plus Z-VAD. These data indicate that autolysosomes were not induced by necroptotic stimulation and that autophagosomes accumulated following TNF-α plus Z-VAD treatment. Thus, necroptotic stimulation may block autophagosome and lysosome fusion. Mature autophagosomes that have acquired STX17 fuse with lysosomes to degrade components [2,28]. STX17-LC3 colocalization was quantified to observe whether TNF-α plus Z-VAD influenced autophagosome–lysosome fusion (Fig. 4B). Cells were transfected with GFP-STX17, and LC3 colocalization was analyzed using microscopy. GFP-STX17 colocalized with LC3 following Torin-1 treatment. However, GFP-STX17 and LC3 colocalization was not enhanced by necroptotic stimulation. These findings indicate that necroptotic stimulation restricts STX17 recruitment. Taken together, these findings suggest that necroptotic stimulation reduced autophagic flux before the autophagosome–lysosome fusion step (Fig. 4C).

Discussion

In the present study, we demonstrate that TNF-α plus Z-VAD stimulation increases LC3 puncta accumulation and SQSTM1/p62 puncta size via RIPK3. These puncta are not aberrant aggresomes induced by the secondary effect of dead cells. Necroptotic stimulation reduced autophagic flux before the autophagosome–lysosome fusion step. These findings provide new insights into the regulation of autophagic flux in dying cells.

Necroptosis is a well-known type of programmed cell death. Previous studies have shown that necroptosis signals induce autophagy [20–24]. Furthermore, several studies have demonstrated that necroptosis signals and autophagy are reciprocal, tightly regulated processes [29,30]. On the other hand, the mechanism of TNF-α stimulation-dependent LC3-II accumulation caused by necroptosis is poorly understood. Previous studies have shown that necroptotic stimulation induces LC3-II in different cell types [20,21,24]. Herein, we showed that necroptosis stimulation (TNF-α plus Z-VAD) increased LC3 puncta in human intestinal epithelial cells (Fig. 1A–E). Our results are consistent with the previous studies that TNF-α induced LC3-II in L929, H9C2, and Jurkat cells. SQSTM1/p62, known as a mediator of selective autophagy, localizes to the cargo and degrades when autophagy flux is increased [3,4]. In contrast, recent work has shown interesting evidence that SQSTM1/p62 expression might be increased following TNF-α plus Z-VAD stimulation [24]. We also observed an increase in SQSTM1/p62 expression after necroptosis stimulation (Fig. 2A–C). Aggresome detection dye further indicates that SQSTM1/p62-LC3-positive structures are not aberrant aggregates (Fig. 3C). We also performed electron microscopy to evaluate the SQSTM1/p62-LC3-positive

structures (data not shown). Surprisingly, we observed an increase in the number of single-membrane structures enclosing the cytoplasmic materials following TNF-α and Z-VAD stimulation. These autophagic vacuoles may be amphisomes. These findings also suggest that necroptotic stimulation reduced autophagic flux before the autophagosome–lysosome fusion step. We will further examine these autophagic vacuoles structures by immunoelectron microscopy in the future.

The necroptosis pathway has been implicated as both an adaptive and pathogenic component of many human diseases involving inflammatory processes, including atherosclerosis, myocardial ischemia, sepsis, inflammatory bowel disease, and neurodegenerative diseases [9]. Several studies have suggested increased activation of autophagy during necroptosis by only the assessment of LC3 accumulation. However, the molecular crosstalk between necroptosis and autophagy remains poorly defined. A recent paper has shown that activated MLKL attenuates autophagy during necroptosis [23]. We provide additional evidence that the accumulation of LC3 occurring during necroptosis is not caused by autophagy activation but by its inhibition. This is very important in the context of inflammation control. Autophagy is critical not only for pathogen clearance but also for cytokine production during inflammation. Our findings caution against how to control inflammation in necroptosis-related diseases and provide critical insights into the regulation of necroptosis and autophagy.

In conclusion, we discovered that TNF-α plus Z-VAD treatment reduces autophagic flux via RIPK3. These findings provide new insights into understanding human diseases involving necroptosis.

Acknowledgments

We thank Masako Akiyama for statistical advice. This study was supported by the Cooperation Program between TMDU and Sony IP&S, Inc. This work was supported by funding from MEXT/JSPS KAKENHI [16K15423, 18K07934, 19H01050]; and the Research Center Network Program for Realization of Regenerative Medicine from AMED [18bm03041h0006, 19bm0304001h0007]. This study was also supported by Naoki Tsuchida Research Grant.

Conflict of interest

The research funding was from Sony Imaging Products & Solutions Inc.

Author contributions

KO performed the majority of experiments and assisted with the manuscript; CM designed and performed the experiments; YN, AT, EA, HM, MK, MO, YN, TN, RO, KT, TN, and ST provided technical assistance; EI and MW supervised experiments; and SO supervised the overall study and wrote the manuscript.

References

1 Morishita H and Mizushima N (2019) Diverse cellular roles of autophagy. *Annu Rev Cell Dev Biol* **35**, 453–475.
2 Itakura E, Kishi-Itakura C and Mizushima N (2012) The hairpin-type tail-anchored SNARE syntaxin 17 targets to autophagosomes for fusion with endosomes/lysosomes. *Cell* **151**, 1256–1269.
3 Sánchez-Martín P, Saito T and Komatsu M (2019) p62/SQSTM1: 'Jack of all trades' in health and cancer. *FEBS J* **286**, 8–23.
4 Kirkin V and Rogov VV (2019) A diversity of selective autophagy receptors determines the specificity of the autophagy pathway. *Mol Cell* **76**, 268–285.
5 Nibe Y, Oshima S, Kobayashi M, Maeyashiki C, Matsuzawa Y, Otsubo K, Matsuda H, Aonuma E, Nemoto Y, Nagaishi T *et al.* (2018) Novel polyubiquitin imaging system, PolyUb-FC, reveals that K33-linked polyubiquitin is recruited by SQSTM1/p62. *Autophagy* **14**, 347–358.
6 He S, Wang L, Miao L, Wang T, Du F, Zhao L and Wang X (2009) Receptor interacting protein kinase-3 determines cellular necrotic response to TNF alpha. *Cell* **137**, 1100–1111.
7 Cho YS, Challa S, Moquin D, Genga R, Ray TD, Guildford M and Chan FK (2009) Phosphorylation-driven assembly of the RIP1-RIP3 complex regulates programmed necrosis and virus-induced inflammation. *Cell* **137**, 1112–1123.
8 Zhang DW, Shao J, Lin J, Zhang N, Lu BJ, Lin SC, Dong MQ and Han J (2009) RIP3, an energy metabolism regulator that switches TNF-induced cell death from apoptosis to necrosis. *Science* **325**, 332–336.
9 Choi ME, Price DR, Ryter SW and Choi AMK (2019) Necroptosis: a crucial pathogenic mediator of human disease. *JCI Insight* **4**, e128834. https://doi.org/10.1172/jci.insight.128834.
10 Newton K, Dugger DL, Wickliffe KE, Kapoor N, de Almagro MC, Vucic D, Komuves L, Ferrando RE, French DM, Webster J *et al.* (2014) Activity of protein kinase RIPK3 determines whether cells die by necroptosis or apoptosis. *Science* **343**, 1357–1360.
11 Takahashi N, Vereecke L, Bertrand MJ, Duprez L, Berger SB, Divert T, Gonçalves A, Sze M, Gilbert B, Kourula S *et al.* (2014) RIPK1 ensures intestinal

homeostasis by protecting the epithelium against apoptosis. *Nature* **513**, 95–99.
12 Newton K, Wickliffe KE, Dugger DL, Maltzman A, Roose-Girma M, Dohse M, Kőműves L, Webster JD and Dixit VM (2019) Cleavage of RIPK1 by caspase-8 is crucial for limiting apoptosis and necroptosis. *Nature* **574**, 428–431.
13 Cuchet-Lourenço D, Eletto D, Wu C, Plagnol V, Papapietro O, Curtis J, Ceron-Gutierrez L, Bacon CM, Hackett S, Alsaleem B *et al.* (2018) Biallelic RIPK1 mutations in humans cause severe immunodeficiency, arthritis, and intestinal inflammation. *Science* **361**, 810–813.
14 Li Y, Führer M, Bahrami E, Socha P, Klaudel-Dreszler M, Bouzidi A, Liu Y, Lehle AS, Magg T, Hollizeck S *et al.* (2019) Human RIPK1 deficiency causes combined immunodeficiency and inflammatory bowel diseases. *Proc Natl Acad Sci USA* **116**, 970–975.
15 Wertz IE, O'Rourke KM, Zhou H, Eby M, Aravind L, Seshagiri S, Wu P, Wiesmann C, Baker R, Boone DL *et al.* (2004) De-ubiquitination and ubiquitin ligase domains of A20 downregulate NF-kappaB signalling. *Nature* **430**, 694–699.
16 Hitotsumatsu O, Ahmad RC, Tavares R, Wang M, Philpott D, Turer EE, Lee BL, Shiffin N, Advincula R, Malynn BA *et al.* (2008) The ubiquitin-editing enzyme A20 restricts nucleotide-binding oligomerization domain containing 2-triggered signals. *Immunity* **28**, 381–390.
17 Onizawa M, Oshima S, Schulze-Topphoff U, Oses-Prieto JA, Lu T, Tavares R, Prodhomme T, Duong B, Whang MI, Advincula R *et al.* (2015) The ubiquitin-modifying enzyme A20 restricts ubiquitination of the kinase RIPK3 and protects cells from necroptosis. *Nat Immunol* **16**, 618–627.
18 Bialik S, Dasari SK and Kimchi A (2018) Autophagy-dependent cell death – where, how and why a cell eats itself to death. *J Cell Sci* **131**, https://doi.org/10.1242/jcs.215152.
19 Galluzzi L, Vitale I, Aaronson SA and Kroemer G (2018) Molecular mechanisms of cell death: recommendations of the Nomenclature Committee on Cell Death 2018. *Cell Death Differ* **25**, 486–541.
20 Degterev A, Huang Z, Boyce M, Li Y, Jagtap P, Mizushima N, Cuny GD, Mitchison TJ, Moskowitz MA and Yuan J (2005) Chemical inhibitor of nonapoptotic cell death with therapeutic potential for ischemic brain injury. *Nat Chem Biol* **1**, 112–119.
21 Ye YC, Yu L, Wang HJ, Tashiro S, Onodera S and Ikejima T (2011) TNFα-induced necroptosis and autophagy via suppression of the p38-NF-κB survival pathway in L929 cells. *J Pharmacol Sci* **117**, 160–169.
22 Lin SY, Hsieh SY, Fan YT, Wei WC, Hsiao PW, Tsai DH, Wu TS and Yang NS (2018) Necroptosis promotes autophagy-dependent upregulation of DAMP and results in immunosurveillance. *Autophagy* **14**, 778–795.
23 Frank D, Vaux DL, Murphy JM, Vince JE and Lindqvist LM (2019) Activated MLKL attenuates autophagy following its translocation to intracellular membranes. *J Cell Sci* **132**, https://doi.org/10.1242/jcs.220996.
24 Ogasawara M, Yano T, Tanno M, Abe K, Ishikawa S, Miki T, Kuno A, Tobisawa T, Muratsubaki S, Ohno K *et al.* (2017) Suppression of autophagic flux contributes to cardiomyocyte death by activation of necroptotic pathways. *J Mol Cell Cardiol* **108**, 203–213.
25 Matsuzawa Y, Oshima S, Nibe Y, Kobayashi M, Maeyashiki C, Nemoto Y, Nagaishi T, Okamoto R, Tsuchiya K, Nakamura T and *et al.* (2015) RIPK3 regulates p62-LC3 complex formation via the caspase-8-dependent cleavage of p62. *Biochem Biophys Res Commun* **456**, 298–304.
26 Yang C, Li J, Yu L, Zhang Z, Xu F, Jiang L, Zhou X and He S (2017) Regulation of RIP3 by the transcription factor Sp1 and the epigenetic regulator UHRF1 modulates cancer cell necroptosis. *Cell Death Dis* **5**, e3084.
27 Thoreen CC, Kang SA, Chang JW, Liu Q, Zhang J, Gao Y, Reichling LJ, Sim T, Sabatini DM and Gray NS (2009) An ATP-competitive mammalian target of rapamycin inhibitor reveals rapamycin-resistant functions of mTORC1. *J Biol Chem* **284**, 8023–8032.
28 Nakamura S and Yoshimori T (2017) New insights into autophagosome-lysosome fusion. *J Cell Sci* **130**, 1209–1216.
29 Harris KG, Morosky SA, Drummond CG, Patel M, Kim C, Stolz DB, Bergelson JM, Cherry S and Coyne CB (2015) RIP3 regulates autophagy and promotes coxsackievirus b3 infection of intestinal epithelial cells. *Cell Host Microbe* **18**, 221–232.
30 Goodall ML, Fitzwalter BE, Zahedi S, Wu M, Rodriguez D, Mulcahy-Levy JM, Green DR, Morgan M, Cramer SD and Thorburn A (2016) The autophagy machinery controls cell death switching between apoptosis and necroptosis. *Dev Cell* **37**, 337–349.